RESEARCH DEPARTMENT

The performance of high-frequency arrays when radiating through other arrays

REPORT No. E-086
1963/33

THE BRITISH BROADCASTING CORPORATION
ENGINEERING DIVISION

RESEARCH DEPARTMENT

THE PERFORMANCE OF HIGH-FREQUENCY ARRAYS WHEN RADIATING THROUGH OTHER ARRAYS

Report No. E-086
(1963/33)

D.J. Whythe, B.Sc.(Eng.), A.M.I.E.E.
P. Knight, B.A., A.M.I.E.E.
K.W.T. Hughes, B.Sc.
J.R. Chew, B.Sc.(Eng.), Grad.I.E.E.

W Proctor Wilson

(W. Proctor Wilson)

This Report is the property of the British Broadcasting Corporation and may not be reproduced in any form without the written permission of the Corporation.

Report No. E-086

THE PERFORMANCE OF HIGH-FREQUENCY ARRAYS WHEN RADIATING THROUGH OTHER ARRAYS

Section Title Page

SUMMARY 1

1. INTRODUCTION 1

2. METHOD OF MEASUREMENT 2

3. MEASUREMENTS WITH OBSTACLES HAVING A KNOWN INSERTION LOSS . 3

- 3.1. An infinite cylindrical wire 3
- 3.2. Rectangular obstacles 3

4. MEASUREMENT OF FIRING-THROUGH LOSS 4

- 4.1. Variation of insertion loss with tuning of obstacle array . . 5
- 4.2. Variation of insertion loss with width of source array 7
- 4.3. Variation of insertion loss with separation between source and obstacle arrays 7
- 4.4. Variation of insertion loss with frequency of the incident radiation 8
- 4.5. The effect of the obstacle array on the vertical radiation pattern of the source array 9
- 4.6. The effect of rotating the obstacle array 9
- 4.7. The effect of lateral displacement of the obstacle 11
- 4.8. The effect of masts and stays 12
- 4.9. The effect of a supporting catenary 13

5. PRACTICAL APPLICATION OF EXPERIMENTAL RESULTS 13

- 5.1. General formula for insertion loss 13
  - 5.1.1. The separation between arrays 14
  - 5.1.2. The number of elements forming the obstacle array . 14
  - 5.1.3. The relative heights of the arrays 14
  - 5.1.4. The relative design frequencies of the arrays . . . 15
  - 5.1.5. The orientation of the obstacle array 17
  - 5.1.6. The h.r.p. of the source array 17

Section Title Page

5.2. Comparison between measured results and curves obtained from the general formula 17
5.3. Variation of insertion loss with position of obstacle 18
5.4. Charts for determining where an obstacle array may be sited . 19
5.5. The insertion loss due to a large number of obstacle arrays . 21

6. THE EFFECT OF IONOSPHERIC IRREGULARITY ON THE INSERTION LOSS OF AN OBSTACLE ARRAY 22

7. CONCLUSIONS 25

8. ACKNOWLEDGEMENTS 25

9. REFERENCES 25

APPENDIX 26

Report No. E-086

September 1963 (1963/33)

THE PERFORMANCE OF HIGH-FREQUENCY ARRAYS WHEN RADIATING THROUGH OTHER ARRAYS

SUMMARY

Measurements are described which have been made to determine the reduction in the distant field strength when obstacles disturb the radiation from a high-frequency curtain array. Experiments were performed with small-scale models, at frequencies in the region of 1100 Mc/s, to measure the disturbance caused by curtain arrays and other obstacles such as stayed masts and support wires.

In general, due to the large number of parameters involved, it is impracticable to deduce a precise value for the insertion loss; an upper limit may however be assessed. Experimental results have been used to derive a general formula, which enables arrays to be sited so that the loss will not exceed a given value.

1. INTRODUCTION

At high-frequency (h.f.) broadcasting stations, large numbers of arrays are required to cater for different service areas and frequency bands. The spacing between them is a matter of some importance because interaction occurs if they are too closely spaced. On the other hand, feeder loss and the amount of land available set an upper limit to their separation. The most serious effect of array interaction is the reduction of field strength which occurs when one array radiates through (or 'fires through') another operating in the same or an adjacent frequency band. This effect is accentuated by the fact that h.f. arrays usually radiate most power at low angles of elevation.

The existence of 'firing-through' loss was demonstrated at the BBC Rampisham station in 1943 by measuring the fields radiated by several arrays while intervening arrays were raised and lowered. Reductions of up to 2·3 dB were observed.[1] The Post Office Engineering Department have performed experiments[2] with models operating at 3000 Mc/s and have determined the insertion loss which occurs when various types of obstacles are placed in front of a rhombic aerial; the experiments using a curtain array were made with the driven curtain terminated in a resistor, and may therefore have been less than the maximum possible. The measured losses were somewhat smaller than the corresponding results described in this report.

In theory it is possible to determine the insertion loss of an obstacle by calculating the currents induced in it, and then finding how the re-radiated field interferes with the direct signal from the source. The mathematical difficulties are such, however, that this method can only be applied to simple obstacles such as infinite wires and rectangular screens. Difficulties arise with arrays of dipoles because the impedances of the dipoles are not equal, and the currents in them can be deduced only by solving a set of simultaneous equations; moreover, some of the mutual impedances between the dipoles are also difficult to calculate. Insertion losses of arrays, therefore, have to be measured experimentally.

This report describes measurements of the insertion loss of curtain arrays of horizontal dipoles, using models operating in the region of 1100 Mc/s. This frequency gives a satisfactory compromise between ease of modelling and the space required to conduct the experiment.

2. METHOD OF MEASUREMENT

The measurements were made by noting the change of amplitude of the received signal when various model obstacles were placed in the path between a model source array and a receiving aerial, as shown in Fig. 1. The receiving aerial should, ideally, have been at a very great distance from the source and the obstacles but, provided the distance is large compared to the separation* between the source and obstacle arrays, the relative fields from the two arrays arrive at the receiving aerial with substantially the correct amplitude and phase relationship. Preliminary experiments indicated that the separations did not need to exceed 40λ (where λ is the wavelength of the radiated signal) since the insertion loss at greater separations was negligible. It was therefore adequate to site the receiving aerial 300λ from the source array since, with separations up to 40λ, negligible error in measurement of insertion loss then resulted.

No attempt was made to model the surface impedance of the ground because results obtained with perfectly-conducting ground approximate very closely to those which would be obtained at full scale over 'practical' ground.

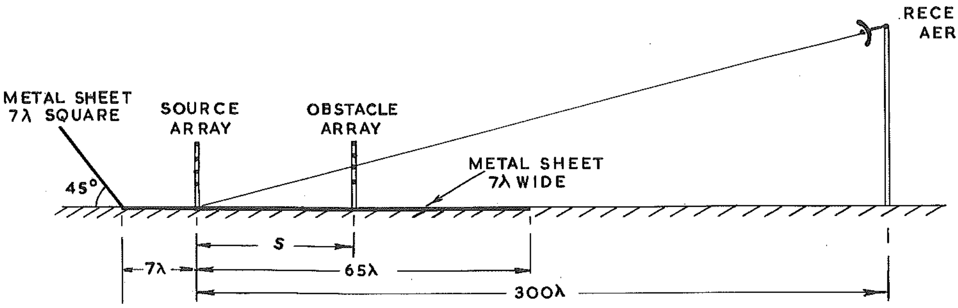

Fig. 1 - Experimental arrangement (not to scale)

---

* As an aid to clarity, the term 'separation' is used throughout this report for the distance between source and obstacle arrays.

In an initial series of experiments, a perfectly-conducting ground plane was simulated by modelling both the source array and its image (which was driven in antiphase), together with the obstacle array and its image. The entire measuring system was suspended above the ground. This method had to be abandoned because unwanted ground reflexions caused considerable errors which could not be avoided. Finally, a level area covered with closely-cut grass was selected as a site for the source and the obstacles. To make the ground reflexion coefficient near to unity, an aluminium sheet 65λ long and 7λ wide was laid on the ground between the test dipole and the receiving aerial; the resulting reflexion coefficient is shown in Fig. 2 together with that obtaining in the absence of the sheet. The addition of the metal sheet increased the reflexion coefficient to a value which approximated closely both in amplitude and phase to that of perfectly-reflecting ground.

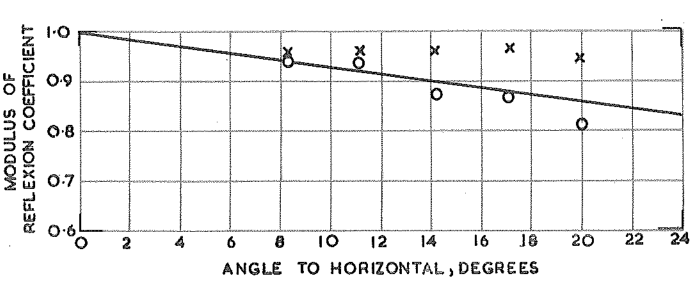

Fig. 2 - Theoretical and measured ground reflexion coefficients

o Values measured without metal sheet laid on ground

— Theoretical curve for ground of average conductivity

× Values measured with metal sheet laid on ground

For perfectly-conducting ground the modulus of the reflexion coefficient is 1·0 for all angles of incidence

It was observed that radiation from behind the source array, when reflected from distant objects such as trees, caused slight amplitude variations of the received signal. These were obviated by mounting an aluminium sheet 7λ square at an angle of 45° behind the array, as shown in Fig. 1.

3. MEASUREMENTS WITH OBSTACLES HAVING A KNOWN INSERTION LOSS

To test the accuracy of the measuring system, measurements were made with obstacles for which the insertion loss could be calculated.

3.1. An infinite cylindrical wire

The insertion loss of an infinite cylindrical wire can be calculated exactly but, for any practical diameter, the insertion loss would have been too small to reveal any sources of error in the measuring system.

3.2. Rectangular obstacles

There is no exact solution for the insertion loss of a rectangular metal obstacle whose dimensions do not greatly exceed the wavelength of the incident radiation. However, an approximate solution sufficiently accurate for the purpose is derived in the Appendix.

Measurements were made with two rectangular metal obstacles whose dimensions were chosen to give losses of the same order of magnitude as those obtained with arrays of dipoles. Fig. 3 shows that reasonable agreement with theory was obtained.

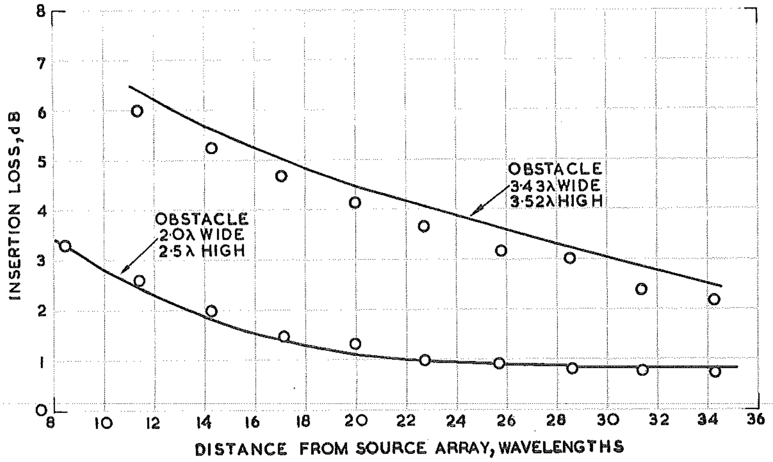

Fig. 3 - The insertion loss of rectangular obstacles

—— Theoretical o Measured

4. MEASUREMENT OF FIRING-THROUGH LOSS

The BBC uses h.f. curtain arrays which consist of tiers of collinear λ/2 elements. The vertical spacing between the rows is λ/2; this enables two columns of λ/2 elements to be end-fed by a single balanced feeder. The arrays are designated Hm/n/h, indicating a horizontally-polarized array of n rows, each comprising m collinear λ/2 elements, the lowest row being hλ above ground. If the array is fitted with a reflector curtain (spaced λ/4 behind the array) the letter 'R' is added to the designation. Thus the term HR2/4/1 designates an array of four rows, each row comprising two collinear λ/2 elements, with a similar curtain spaced horizontally by λ/4 to act as a reflector. As an example, an HR4/4/1 array is shown schematically in Fig. 4.

The model source array was not required to be an accurate model of a full-scale aerial since only its vertical radiation pattern (v.r.p.) was important. On the other hand, the obstacle arrays were required to be modelled as accurately as possible. At full scale, each element usually consists of two parallel wires in order to increase the bandwidth but, to make the elements of the model obstacle arrays stronger and easier to handle, single wires of larger, electrically equivalent, diameter were used. The rows and columns of the model elements, fitted with PTFE insulators and tensioned with nylon string, were mounted in light wooden frames. Since the source impedance of transmitters is predominantly reactive, model feeders, where fitted, were terminated in a short-circuit, the position of which was adjustable. Before using models of arrays with reflector curtains, the short-circuit associated with the reflector curtain was set, as at full scale, at a position which gave minimum radiation in the back direction when radiating from the driven curtain.

The insertion loss of an obstacle array depends upon several factors. The effect of each of these factors was investigated in turn and the results are described in the following sections.

The experiments were performed using an H2/4/1, an H4/4/1 or an H2/2/0·5 source array. The receiving aerial was always located in the vertical plane normal to the source array and, unless otherwise stated, at a height corresponding to the

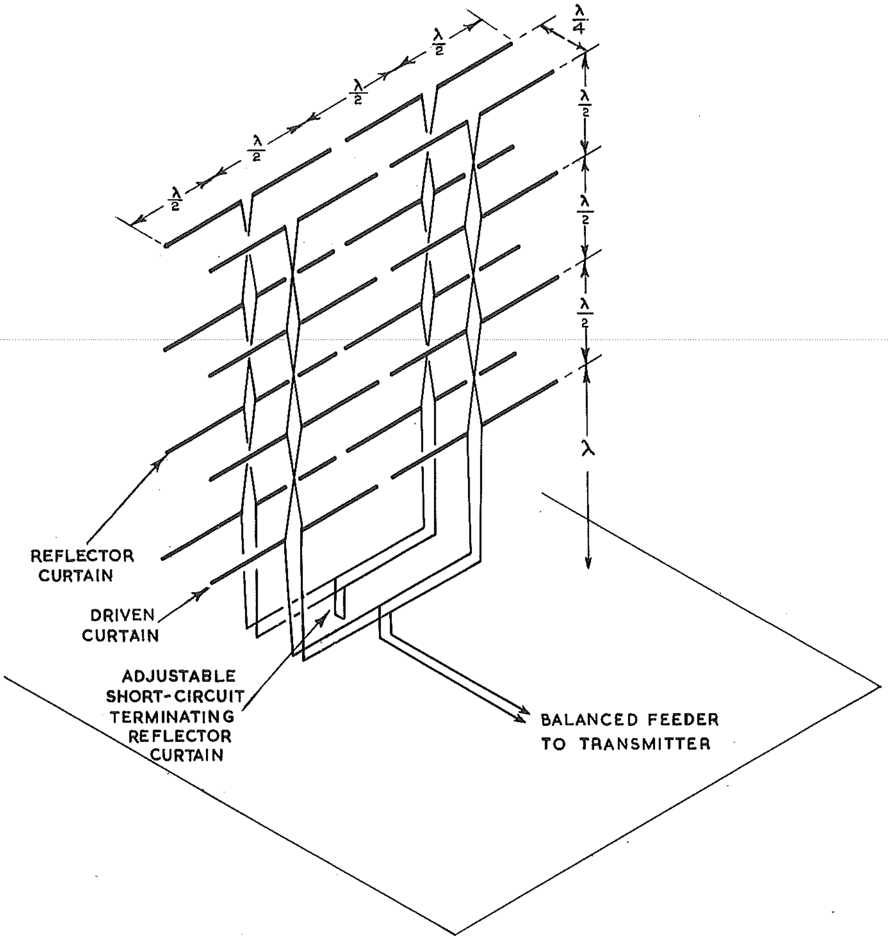
λ/2
λ/2
λ/2
λ/2
λ/2
λ/4
λ/2
λ/2
λ/2
λ
REFLECTOR CURTAIN
DRIVEN CURTAIN
ADJUSTABLE SHORT-CIRCUIT TERMINATING REFLECTOR CURTAIN
BALANCED FEEDER TO TRANSMITTER

Fig. 4 - Schematic diagram of HR4/4/1 array

centre of its main lobe (i.e., at an angle of 7½° to the horizontal when using the H2/4/1 and H4/4/1 source arrays, and at 18° when using the H2/2/0·5 source array). The loss measured in this way is typical of that occurring over a practical transmission path (see Section 4.5.).

4.1. Variation of insertion loss with tuning of obstacle array

Whether or not an obstacle array is connected to a transmitter, it is terminated by an impedance which is predominantly reactive. If its design frequency is the same as that of the incident radiation, a similar terminating reactance is presented to all pairs of elements since the length of each interconnecting feeder is λ/2. Neglecting mutual impedances, it is possible for this reactance to have a value which 'tunes' all the elements of the array, giving rise to a large insertion loss. Fig. 5 shows the variation of insertion loss with terminating reactance when using an H2/4/1 obstacle array at a separation of 17·2λ from an H2/4/1 source. As would be expected, the insertion loss is a maximum when the terminating reactance (referred to the feedpoint at the junction of the two λ/2 elements) is infinite, and is a minimum when the terminating reactance is zero.

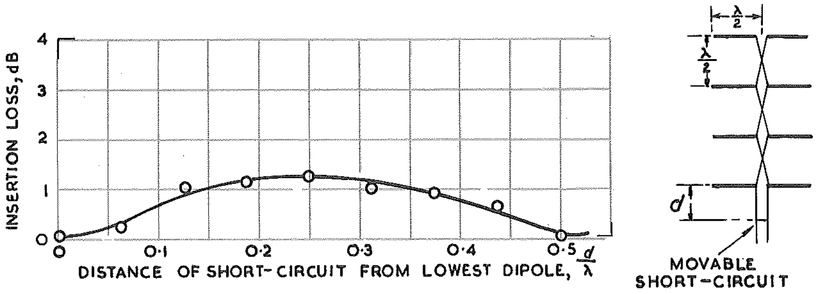

Fig. 5 - The measured insertion loss of an H2/4/1 obstacle array terminated by a variable reactance

Separation between arrays 17·2λ

At the large separation used to obtain the results shown in Fig. 5, equal co-phased voltages were induced in all the elements of the obstacle and thus, when the stub was adjusted for maximum loss, no current flowed in the interconnecting feeders. With much smaller separations, unequal voltages will be induced in each element; currents will then flow in the interconnecting feeders, however, such as to make the currents at the centres of the elements equal and co-phased. Irrespective of the separation, therefore, the v.r.p. of the re-radiation from the obstacle is the same as if it were driven.

If the v.r.p. of the source differs from that of the obstacle array the insertion loss may be small. This effect is illustrated in Fig. 6, curve (a), which shows the insertion loss of an H4/4/1 obstacle at various separations from an H2/2/0·5 source array driven at the design frequency of the obstacle. Fig. 6, curve (b) shows that the insertion loss is considerable when interconnecting feeders are omitted, and the v.r.p. is consequently modified; thus the presence of feeders can greatly affect the insertion loss of an array. For all subsequent measurements, unless otherwise stated, the obstacles were fitted with feeders and an adjustable short-circuited stub.

Experiments showed that the variation of insertion loss with tuning was not always as broad as shown in Fig. 5. For example, Fig. 7 shows a rapid variation of insertion loss with tuning for an H4/4/1 obstacle at a separation of 11·5λ from an

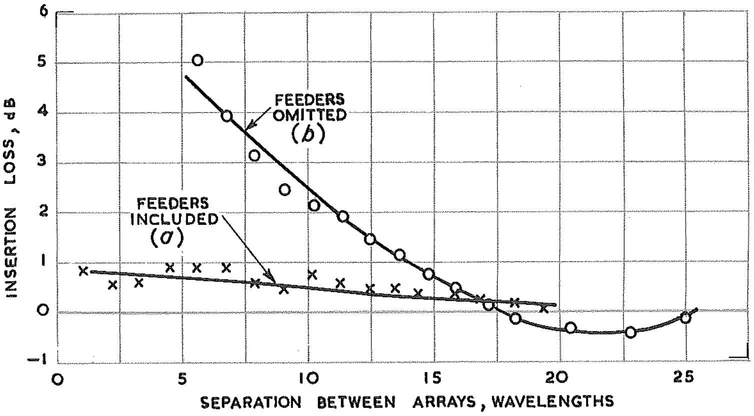

Fig. 6 - Insertion loss of an H4/4/1 obstacle array in the path of an H2/2/0·5 source array

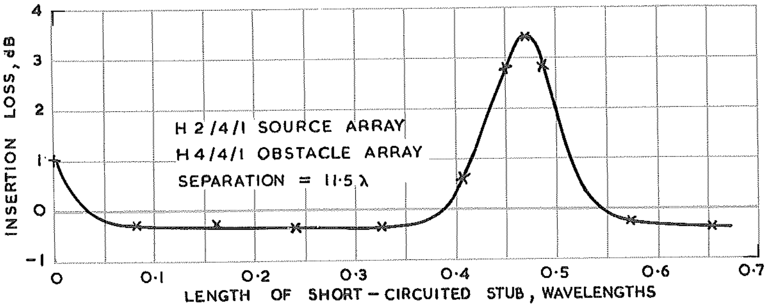

Fig. 7 - Variation of insertion loss with changes of stub-length when the design frequency of the obstacle is 0·93 times the frequency of the incident radiation

H2/4/1 source array; in this case the radiating frequency was 0·93 times the design frequency of the obstacle. Unless otherwise stated, all the results quoted in this report refer to the condition giving the maximum insertion loss.

4.2. Variation of insertion loss with width of source array

If, when the source, the obstacle and the observer are in line, the width of the source array is changed, the distant field, as well as the current in each element of the obstacle, is changed by very nearly the same factor. The relative amplitude of the field re-radiated by the obstacle therefore remains substantially unchanged. This result was verified experimentally using an H2/4/1 or an H4/4/1 array as the source together with an H2/4/1 or an H2/2/0·5 array as the obstacle. At the design-frequency of the obstacles, the insertion loss of each obstacle was found to be substantially independent of the width of the source over the range of separations from 5λ to 35λ. On the other hand, a 'ripple' was observed on the experimental results which was dependent on the source employed; a similar ripple is apparent on the results shown in Fig. 6. By a separate series of experiments, the ripple was shown to be due to re-radiation by the source array of part of the reflected field from the obstacle. The apparent period of the ripples shown in Fig. 6 is greater than the true period because of the relatively large interval between measured points. Such ripples are only likely to be significant when the obstacle is parallel to, and sited near to the line normal to the source array. Since obstacles are seldom sited in that way in practice, smoothed curves have been drawn through the measured points and the ripples disregarded.

4.3. Variation of insertion loss with separation between source and obstacle arrays

The insertion loss of H2/2/0·5, H2/4/1, H4/4/1 and HR4/4/1 obstacles was measured when using an H2/2/0·5 and an H4/4/1 source array. Measurements were made at separations where the insertion loss was appreciable, but not at separations where the loss was greater than about 4 dB (any greater loss would be regarded as unacceptable in practice). The results are shown in Figs. 8 and 9; the insertion loss of the HR4/4/1 obstacle was found to be substantially unchanged if it was rotated through 180°.

The measurements were made only at the frequency for which the obstacles were designed; the variation of insertion loss with separation at other frequencies can be assessed from the results given in the next section.

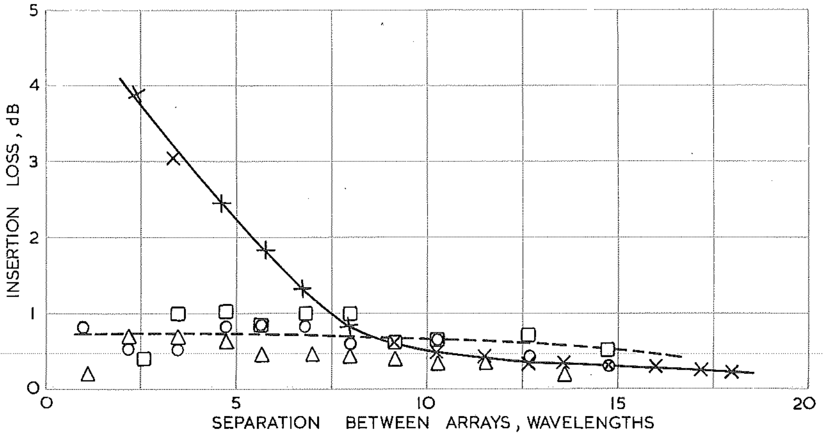

Fig. 8 - Insertion loss of obstacle arrays at various separations from an H2/2/0·5 source array

× H2/2/0·5 obstacle
△ H2/4/1 obstacle
○ H4/4/1 obstacle
□ HR4/4/1 obstacle

4.4. Variation of insertion loss with frequency of the incident radiation

The measurements so far described have been confined primarily to obstacle arrays designed for the same frequency as that of the incident radiation. Although these would be expected to produce the largest insertion losses, the possibility that arrays of other sizes will produce appreciable losses cannot be disregarded. The frequencies of the transmissions from BBC short-wave stations extend over a range of about 6 : 1, and to cover all possible combinations would present a formidable task. Fortunately, however, it was found necessary to measure the insertion loss of each obstacle over a frequency range of only about 2 : 1.

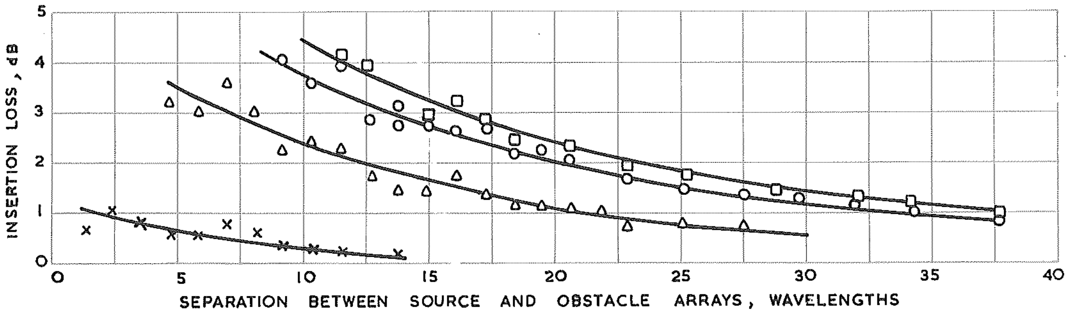

Fig. 9 - Insertion loss of obstacle arrays at various separations from an H4/4/1 source array

× H2/2/0·5 obstacle
△ H2/4/1 obstacle
○ H4/4/1 obstacle
□ HR4/4/1 obstacle

To avoid making a large number of obstacle arrays, models were made with design frequencies 0, ± 15% and ± 30% relative to that of the incident radiation, and results for intermediate frequencies were obtained by varying the frequency of measurement. Using an H2/4/1 source array, the insertion losses of H4/4/1 obstacles were measured at separations of 6λ, 11·5λ and 17·2λ; the losses of HR4/4/1 obstacles were measured at a separation of 18·3λ. The maximum loss obtainable with each obstacle as the length of tuning stub was varied (see Section 4.1) is shown in Figs. 10 and 11. As before, the loss of the HR4/4/1 arrays was substantially unchanged if the obstacles were rotated through 180°.

Figs. 10 and 11 show that the insertion loss becomes small when the frequency of the incident radiation differs by ± 40% from the design frequency of the obstacle. If the frequency of the incident radiation be further reduced, the insertion loss will remain small because the elements forming the obstacle array cannot again become resonant.* If the frequency of the incident radiation be increased, however, further maxima may occur at frequencies which correspond to odd multiples of the obstacle design frequency. This effect is further discussed in Section 5.1.4.

4.5. The effect of the obstacle array on the vertical radiation pattern of the source array

The presence of the obstacle modifies the v.r.p. of the source array. The resulting v.r.p. was deduced by measuring insertion losses at various angles of elevation and subtracting them from the pattern of an unobstructed source. Measurements were made using an H4/4/1 source array and HR4/4/1 obstacles, with separations between source and obstacle of 10λ, 17·2λ and 25λ. The insertion losses of obstacles designed for frequencies equal to, 15% higher and 15% lower than that of the incident radiation were measured. The results, shown in Fig. 12, were obtained with the short-circuited stub on each model set at the position which gave maximum insertion loss at an elevation of 7½°.

Because of the different possible transmission modes, the signal received from a high-frequency array at a distant receiving point is the sum of several components, propagated by different modes. Assuming that these contributions add in random phase, the received power is proportional to the r.m.s. sum of the separate components. The effective insertion loss of the obstacles calculated in this way over ranges of elevations centred about the main lobe is found to be substantially independent of the range of elevations, and equal to the loss measured at the centre of the main lobe. Throughout this report, therefore, the effective insertion loss is taken to be that measured at the centre of the main lobe, and all the results so far discussed are for that condition.

4.6. The effect of rotating the obstacle array

When the plane of the obstacle is not normal to the line joining it to the source, the voltages induced in the columns of elements forming the obstacle will not be co-phased. If the obstacle comprises more than two columns of elements, the relative phases of the associated currents will depend upon both the angle of rotation of the obstacle and the length of the base feeders which join its columns.

---

* It is true that the elements of an array comprising a single row of dipoles would resonate if they were terminated in a short-circuit and illuminated at one-half their design frequency. The insertion loss of such an array, however, is not likely to be very great due to its low height (usually λ/4).

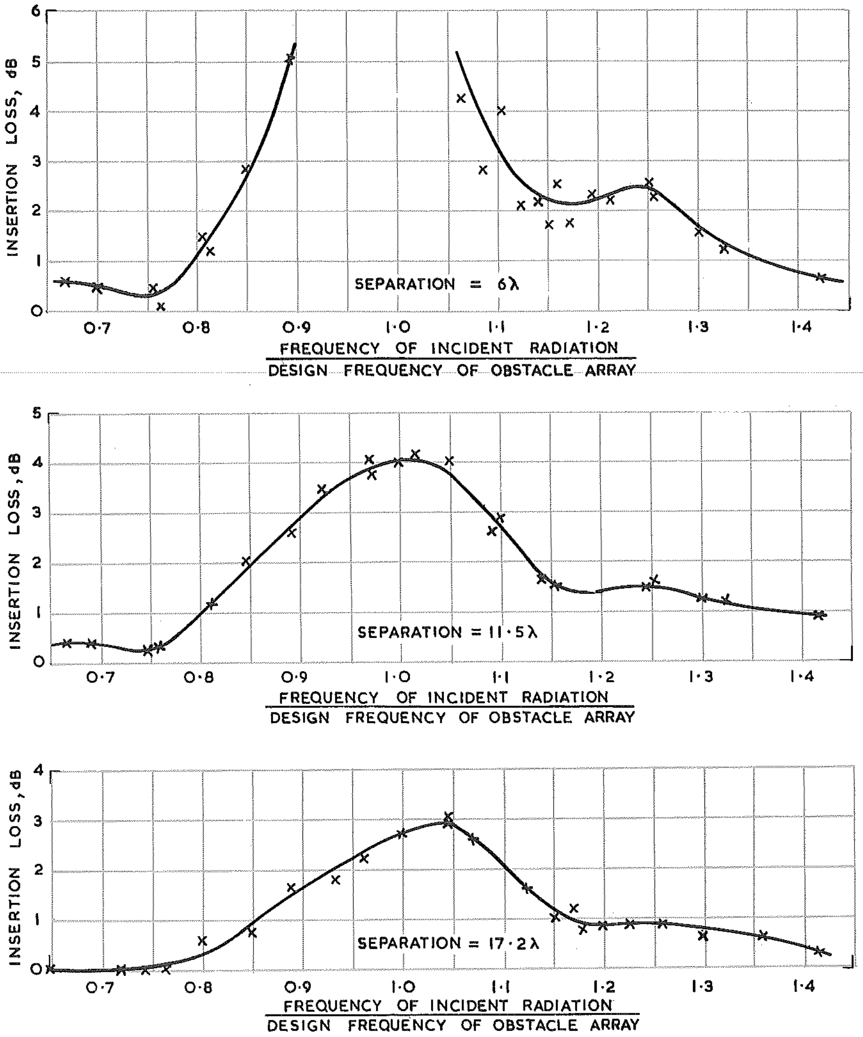

Fig. 10 - Maximum insertion loss of H4/4/1 obstacle array in the path of an H4/4/1 source array radiating at various frequencies

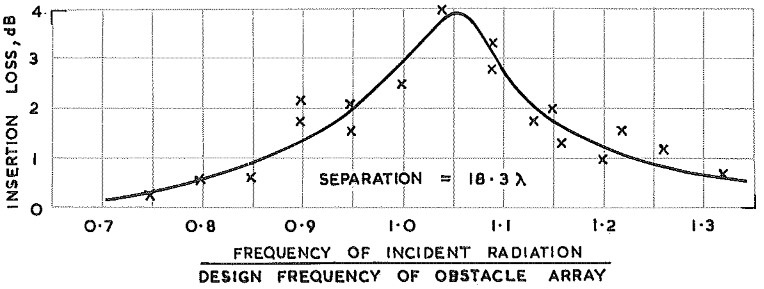

Fig. 11 - Maximum insertion loss of HR4/4/1 obstacle in the path of an H4/4/1 source array radiating at various frequencies

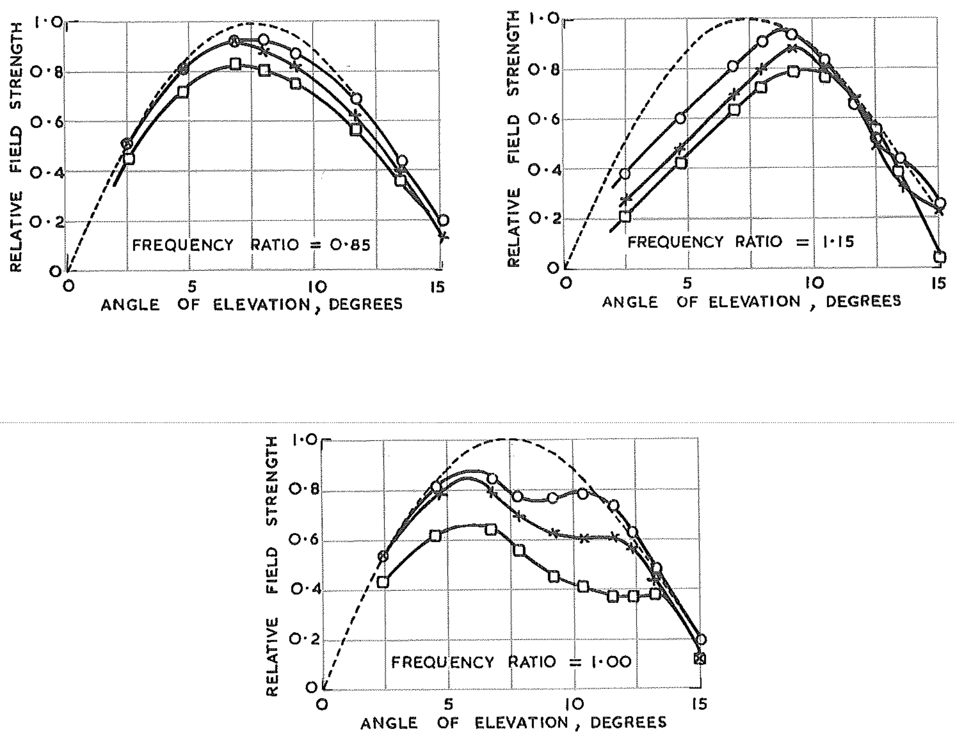

Fig. 12 - Modified v.r.p. of H4/4/1 source array due to HR4/4/1 obstacle arrays of various design frequencies at various separations

$$\text{Frequency ratio} \equiv \frac{\text{frequency of incident radiation}}{\text{design frequency of obstacle array}}$$

□	10λ	separation between arrays
×	17·2λ	separation between arrays
○	25λ	separation between arrays
- - - - -		unmodified v.r.p.

Obstacle arrays tuned for maximum loss at 7½° elevation

Without base feeders, the maximum re-radiation from the obstacle would be expected to occur along the direction of the incident radiation and to be proportional to $\cos^2\psi$, where ψ is the angular rotation of the obstacle as shown in Fig. 13; this was confirmed by experiment. With base feeders, the maximum re-radiation may occur at any bearing between the direction of the incident radiation and the direction of the normal to the array. If the length of the base feeders is such that the maximum re-radiation occurs along the direction of the normal to the array, it can increase to a value proportional to $\cos\psi$. These two cases are shown in Fig. 13.

4.7. The effect of lateral displacement of the obstacle

When an obstacle is moved laterally away from the line normal to the source array, the phase of the re-radiated field changes as the path length from the source increases. When the path length has increased by an odd number of half-wavelengths, the re-radiated field augments the direct field instead of opposing it. The fact that an obstacle array can, under certain circumstances, increase the distant field strength is, however, disregarded in this report because an increase in one direction is likely to be accompanied by a decrease in another equally important direction.

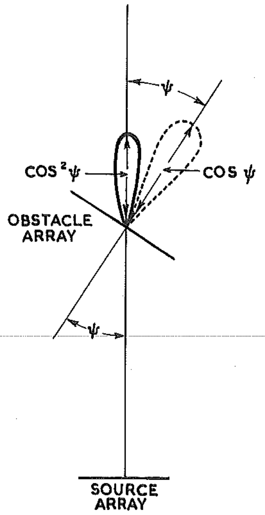

Fig. 13 - Effect of rotating the obstacle array

4.8. The effect of masts and stays

The masts which support the arrays at BBC stations are about 6 ft (2 m) wide and, being small compared even with the shortest wavelength, they have a negligible effect on the distant field strength. Some insertion loss may, however, be caused by the stay wires.

The insertion loss which would be caused by a stayed mast was investigated with models 3·7λ and 7·4λ high corresponding, at mid-band, to typical 250 ft (76 m) and 500 ft (152 m) masts of the type used at short-wave stations. Each of these was provided with twelve stays attached at three different levels, the normal arrangement for masts of square cross-section. The stays, as at full scale, were not broken electrically by insulators, and care was taken to ensure that good contact was established between the stays and the ground plane. The obstacle masts were oriented as shown in Fig. 14, which also shows the results obtained over a range of separations when using an H2/4/1 source array. The effect of lateral displacement was investigated and found to be similar to that for an obstacle array (see Section 4.7.).

The results imply that the insertion loss is greatest when a point roughly one third up from the base of the mast is most strongly illuminated by the source and that the loss is then less than 1 dB. The loss is roughly halved when one set of stays is parallel to the plane containing the source array.

Self-supporting towers, such as those at the BBC Daventry station, may offer appreciable obstruction, especially at the higher frequencies. For negligible loss, they should be separated by about 1000 ft (300 m) from low-angle source arrays such as H4/4/1, or by about 500 ft (150 m) from high-angle source arrays such as H2/2/0·5.

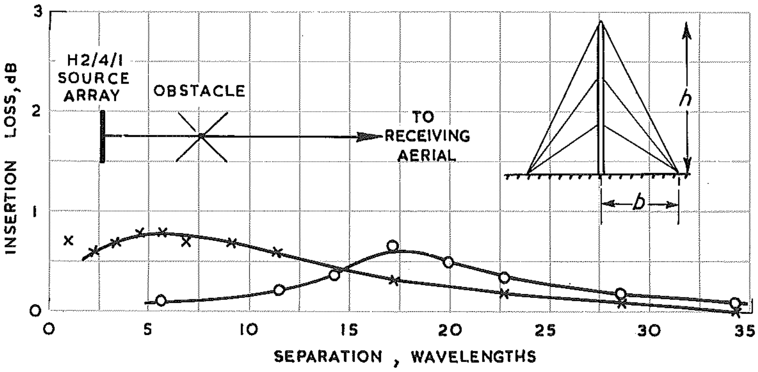

Fig. 14 - The measured insertion loss of a stayed mast

× $h = 3{\cdot}7\lambda$, $b = 2{\cdot}2\lambda$

o $h = 7{\cdot}4\lambda$, $b = 4{\cdot}4\lambda$

4.9. The effect of a supporting catenary

The catenaries from which high-frequency arrays are suspended are usually divided by insulators into sections which are very much shorter than the wavelength of the array they support. However, the length of these sections may be comparable with the wavelength of the incident radiation when the array becomes an obstacle. Some reduction in field strength may then occur, especially when the sections are about $\lambda/2$ long. A long wire divided by insulators into 23 equal sections each $0{\cdot}42\lambda$ long was placed $2{\cdot}3\lambda$ above the ground (corresponding, at mid-band, to a height of about 150 ft (46 m)) in front of an H4/4/1 array at a separation of $17{\cdot}2\lambda$. The insertion loss was measured over a small range of frequencies to simulate the effect of changing the length of the sections. Fig. 15 shows that the loss is greatest when the length of each section is about $0{\cdot}4\lambda$, whereas this condition would be expected to occur for a length of $0{\cdot}5\lambda$. The difference is probably due to the capacitance across the insulators which makes the electrical length greater than $0{\cdot}4\lambda$.

5. PRACTICAL APPLICATION OF EXPERIMENTAL RESULTS

Except for a few special cases, the experimental results described in Section 4 are not in a convenient form for direct application to practical problems. It is, however, possible to derive a general formula from them, based partly on the experimental results and partly on theoretical considerations. This is preferable to an entirely empirical formula since it is less likely to fail when used outside the range of the measurements.

5.1. General formula for insertion loss

When the presence of an obstacle causes a reduction of field strength, the re-radiated field is approximately in antiphase with the direct field. In these circumstances, the insertion loss in decibels, L, is given approximately by the equation:

$$L = 20 \log_{10} \frac{1}{1-u} \tag{1}$$

where u is the ratio, at the distant point of observation, of the re-radiated and direct fields. This expression forms the basis for the general formula.

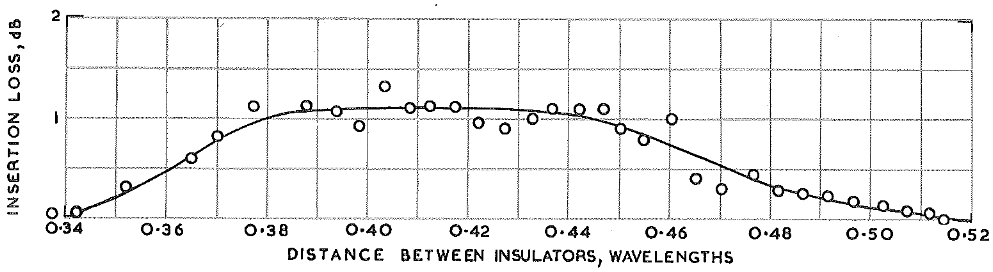

Fig. 15 - The measured insertion loss of a wire broken by insulators. Distance from source array 17·2λ

The relative amplitude of the re-radiated field, u, depends upon the following factors:

(i) The separation between the obstacle and source arrays.

(ii) The number of elements forming the obstacle array.

(iii) The relative heights of the source and obstacle arrays.

(iv) The design frequency of the obstacle array relative to that of the incident radiation.

(v) The angle between the normal to the obstacle array and the direction of the incident radiation.

(vi) The horizontal radiation pattern (h.r.p.) of the source array.

Each of these factors influences the value of u as follows:

5.1.1. The separation between arrays

The currents induced in, and therefore the field re-radiated by, an obstacle very close to the source would be expected to vary inversely as the square root of the separation between the two arrays. At moderate distances the current would be expected to vary inversely with the separation. At great distances, due to interference between rays from the source and its image, it would vary inversely with the square of the separation. Thus the re-radiated field was assumed to be proportional to $1/(\mathbf{A}(s)^{1/2} + \mathbf{B}s + \mathbf{C}s^2)$ where s is the separation between the arrays (expressed in wavelengths at the frequency of the incident radiation) and $\mathbf{A}$, $\mathbf{B}$ and $\mathbf{C}$ are constants. It was found that a good overall fit to the curves could be obtained by the choice: $\mathbf{A} = 4{\cdot}5$, $\mathbf{B} = 2{\cdot}3$ and $\mathbf{C} = 0{\cdot}032$.

5.1.2. The number of elements forming the obstacle array

The re-radiated field is assumed to be proportional to the number of columns of elements forming the obstacle array. Inspection of the insertion loss of H2/4/1 and H4/4/1 obstacles shown in Fig. 9 shows this to be approximately true. The re-radiated field of each obstacle is also assumed to be proportional to the number of rows of elements which it contains.

It can be shown theoretically that the addition of a correctly-tuned reflector will, at its design frequency, make only a small difference to the insertion loss of an array. As shown in Fig. 9, this was confirmed experimentally in one case by using H4/4/1 and HR4/4/1 obstacle arrays. The value of u is therefore taken to be proportional to the number of elements forming the obstacle array, but disregarding those which form a reflector curtain.

5.1.3. The relative heights of the arrays

As mentioned in Section 4.1., the effective insertion loss of an obstacle depends upon the similarity between its v.r.p. and that of the source array. The insertion loss is likely to be greatest when the two patterns are similar because the maximum re-radiation from the obstacle, by coinciding with the main lobe of the source array, occurs along what is usually the optimum propagation path to the distant receiver. If the height of the obstacle in wavelengths is greater than that of the source, the maximum re-radiation occurs below the main lobe of the source, and vice versa. It is impossible to express, by a simple factor, the effect of all the arrays in current use by the BBC, but, for the present purpose, it is sufficient to consider a 'height-equality factor' which is unity when the source and obstacle arrays are of equal height and which is less than unity when the heights of the two arrays are different. The factor, *E*, (shown in Fig. 16) was derived by considering the calculated v.r.p.s of all the arrays in current use by the BBC; it represents the proportion of the maximum re-radiation from the obstacle which occurs at the elevation of the main lobe of the source array. The value of *E* is determined by the ratio of the overall physical heights of the two arrays.

5.1.4. The relative design frequencies of the arrays

The manner in which the insertion loss depends on the design frequency of the obstacle relative to that of the incident radiation cannot be represented by any simple theoretical expression. An empirical factor relating the amplitude of the re-radiated field to the relative frequencies of the obstacle array and the incident radiation was therefore derived from the measured results of Fig. 10. This factor, *F*, is shown in Fig. 17(a) as a function of the frequency ratio. Further maxima of the frequency factor will occur when the frequency of the incident radiation is an odd multiple of the obstacle design-frequency, since the elements forming the obstacle can again become resonant. The empirical curve shown in Fig. 17(b), the maximum value of which is based on theoretical comparisons[3] of the scattering coefficients of wires $\lambda/2$ and $3\lambda/2$ long, may be applied to assess an upper limit for the loss when the frequency of the incident radiation is approximately three times the design frequency of the obstacle. It is unlikely that further maxima need be considered, since either the height-equality factor discussed in Section 5.1.3. will be small or the obstacle will consist of only a single half-wave dipole.

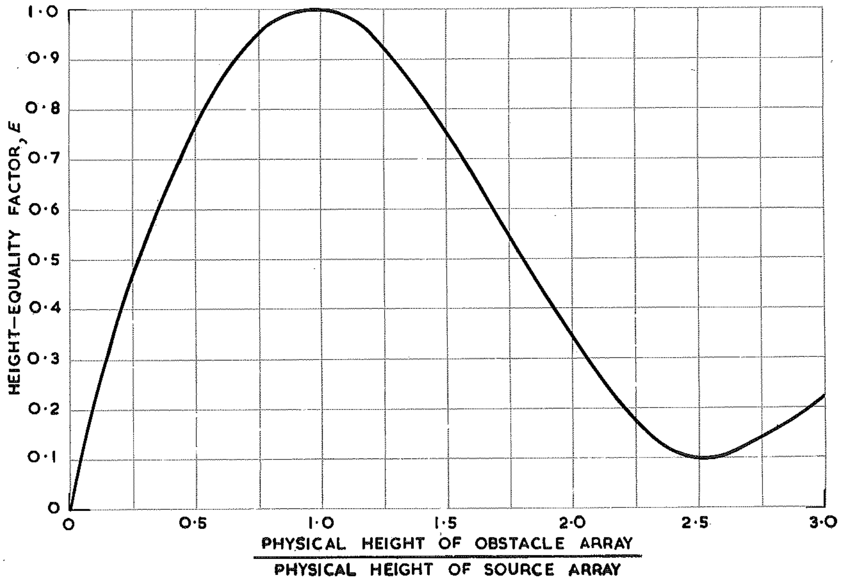

Fig. 16 - Height-equality factor

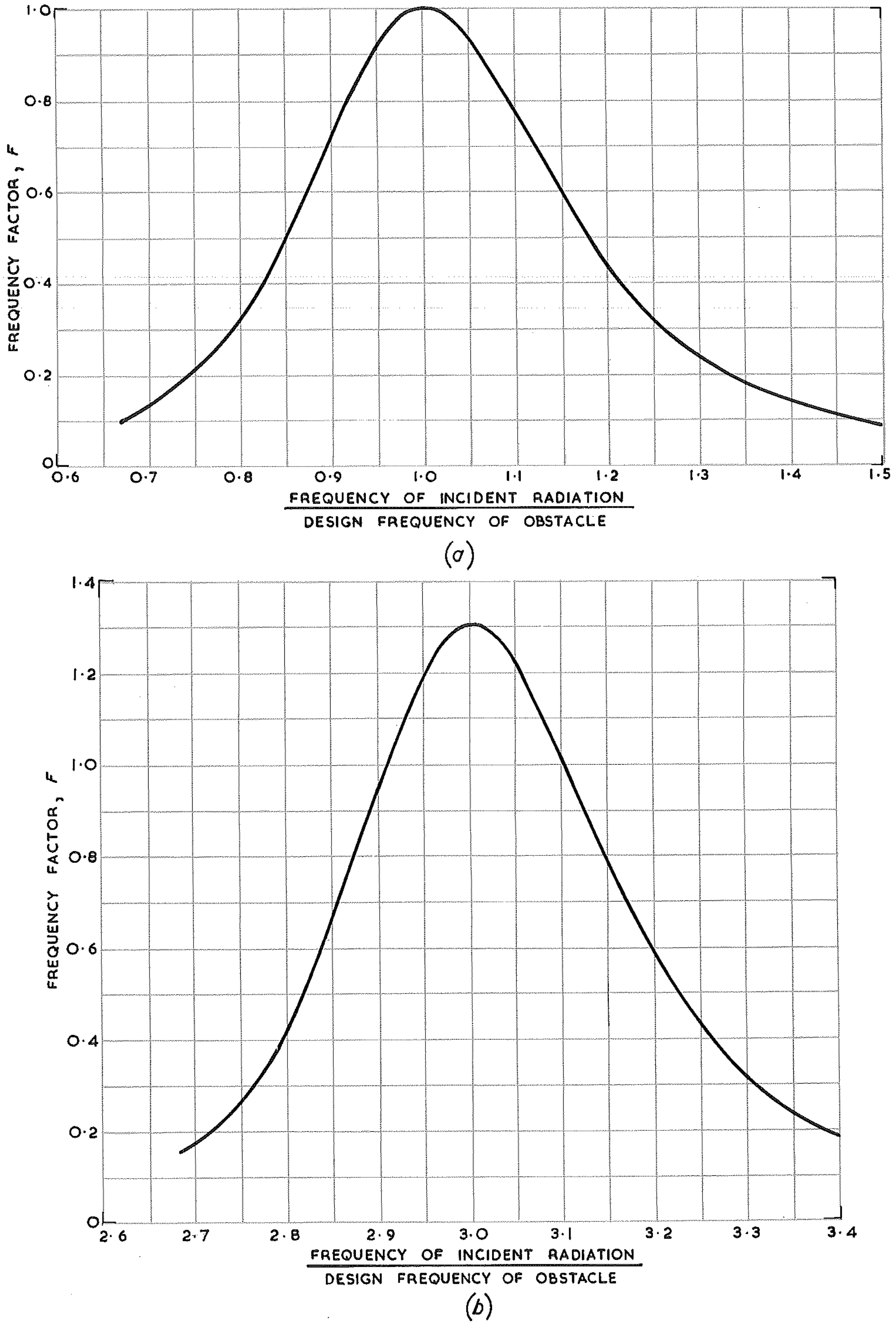

(a)

(b)

Fig. 17 - Frequency factor

5.1.5. The orientation of the obstacle array

The relationship between insertion loss and the angle (ψ) which the normal to the obstacle makes with the direction of the incident radiation was discussed in Section 4.6; the amplitude of the re-radiated field is taken to be proportional to $\cos\psi$ since this is the greatest value that can occur.

5.1.6. The h.r.p. of the source array

If the obstacle and the observer do not lie along the same bearing from the source array, the relative fields radiated along the two bearings (and hence the insertion loss) will depend upon the h.r.p. of the source array. This is expressed as a factor H which is discussed later in Section 5.3.

The complete expression for u in equation (1) is therefore:

$$u = \frac{K}{\left\{4\cdot 5(s)^{1/2} + 2\cdot 3s + 0\cdot 032s^2\right\}} \cdot H \qquad (2)$$

where

$$K = NEF \cos\psi \qquad (3)$$

N is the number of elements forming the obstacle array

E is the height-equality factor given in Fig. 16.

F is the frequency factor given in Fig. 17.

ψ is the angle between the normal to the obstacle and the direction of the incident radiation shown in Fig. 13.

s is the separation between the source and obstacle arrays expressed in wavelengths of the incident radiation.

H is the factor depending upon the h.r.p. of the source array. This is discussed later in Section 5.3.

5.2. Comparison between measured results and curves obtained from the general formula

The measured results shown in Figs. 8 and 9 are compared with the corresponding curves derived from the general formula (for which E, F, H, and $\cos\psi$ are each unity) in Figs. 18 and 19. The measured results of Fig. 10 are compared with the corresponding calculated curves (for which E, H and $\cos\psi$ are each unity) in Fig. 20. The agreement is fairly good; a more stringent test is to compare the calculated curves with measured results other than those by which the general formula was obtained. Such a comparison is given in Fig. 21 (where F, H and $\cos\psi$ are each unity) and in Fig. 22 (where E, H and $\cos\psi$ are each unity). Again, reasonable agreement is obtained.

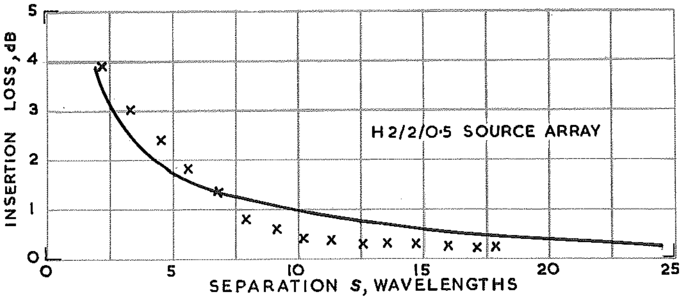

Fig. 18 - Comparison of measured loss and curves derived from the general formula, using an H2/2/0·5 obstacle array designed for the frequency of the incident radiation

x measured points
— curve calculated from general formula

5.3. Variation of insertion loss with position of obstacle

If the source, obstacle and observer are not in a direct line, the insertion loss is modified by a factor, *H*, which depends on the h.r.p. of the source array. As discussed in Section 4.6., the horizontal re-radiation pattern of the obstacle depends upon the length of the base feeders connecting the columns of radiating elements. Depending upon this length, the maximum re-radiation will occur in a direction between the normal to the array and the direction of the incident radiation. In Fig. 23, the obstacle array is shown sited in the direction ϕ from the source array and oriented at angle ψ. The maximum re-radiation from the obstacle may occur in any direction over the range ψ as shown. The greatest insertion loss is caused when the maximum occurs along the direction θ towards the observer. The value of ψ may be such as to prevent this happening in some cases, but the following calculations, to determine an upper limit for the insertion loss, assume that it occurs in all cases.

The factor by which the insertion loss of an obstacle must be modified is the ratio of the fields radiated towards the obstacle and towards the observer. This ratio, *H*, is shown in Fig. 24 for source arrays $\lambda/2$, λ and 2λ wide, for observers at various bearings between the half-power points of the source array.

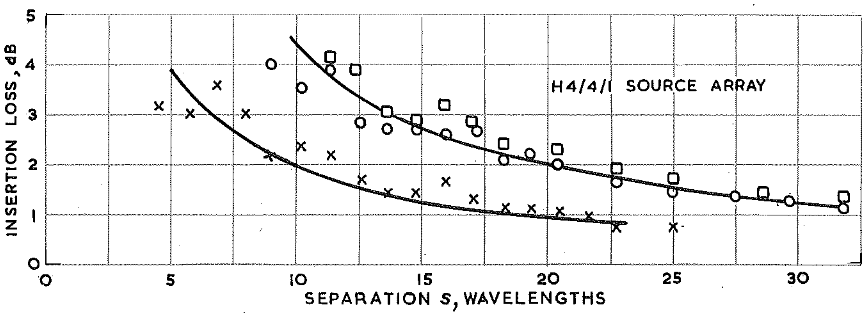

Fig. 19 - Comparison of measured loss and curves derived from the general formula, using obstacle arrays designed for the frequency of the incident radiation

× measured points for H2/4/1 obstacle
○ measured points for H4/4/1 obstacle
□ measured points for HR4/4/1 obstacle
— curve calculated from general formula

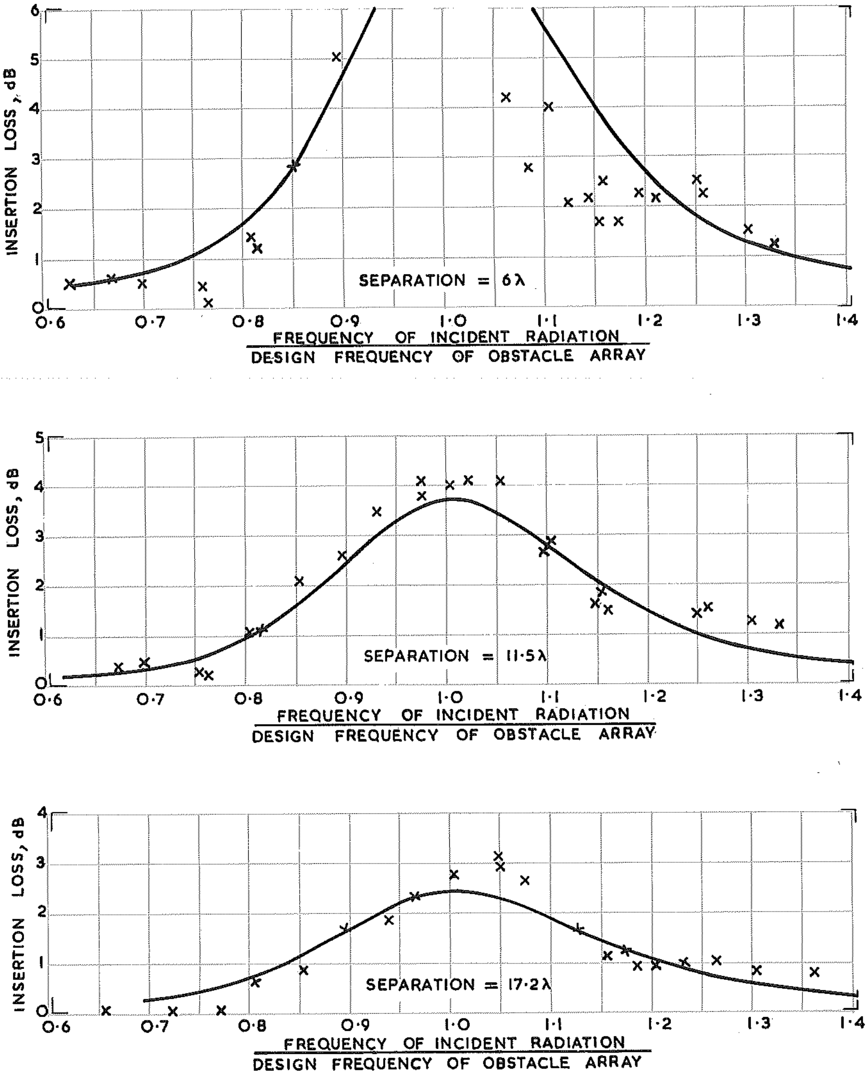

Fig. 20 - Comparison of measured loss and curves derived from the general formula; H4/4/1 obstacle arrays used at various frequencies with an H4/4/1 source array

× measured points
—— general curve

At bearings corresponding to the half-power points of the source array, the re-radiated field from the obstacle is likely to cause a larger loss than in the direction normal to the array since the direct signal along those bearings is weaker. Thus, to assess the maximum insertion loss that an obstacle may cause at bearings between the half-power points, the value of H should be taken from the curve which has the value $(2)^{\frac{1}{2}}$ at $\phi = 0$.

5.4. Charts for determining where an obstacle array may be sited

For the values of insertion loss which are of interest ($L < 4$ dB) equation (1) may be replaced by the approximate formula:

$$L = 10u \qquad (4)$$

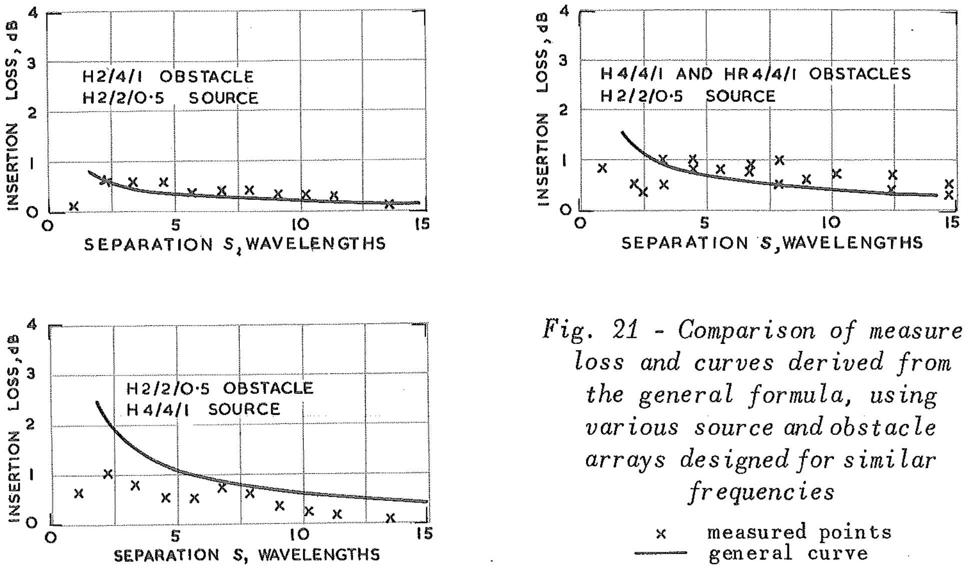

Fig. 21 - Comparison of measured loss and curves derived from the general formula, using various source and obstacle arrays designed for similar frequencies

× measured points
—— general curve

Combining this with equation (2), and re-arranging, gives:

$$4{\cdot}5(s)^{1/2} + 2{\cdot}3s + 0{\cdot}032s^2 = 10H.\frac{K}{L} \qquad (5)$$

This is a quartic equation in s which enables the necessary separation between arrays (s) to be determined in terms of the obstacle parameters (K), the maximum permissible loss (L) and the factor (H) which depends on the h.r.p. of the source array.

The most convenient way to indicate values of s is by means of contour maps for constant values of K/L; maps for three types of source array are shown in Figs. 25 to 27. The maps, drawn for H1/n/h, H2/n/h, and H4/n/h source arrays, take account of loss due only to the obstacle array itself and show the maximum loss likely to occur at any bearing between the half-power points of the source array. If losses due to masts, stays and supporting wires are appreciable, a separate allowance must be made as outlined in Sections 4.8. and 4.9.

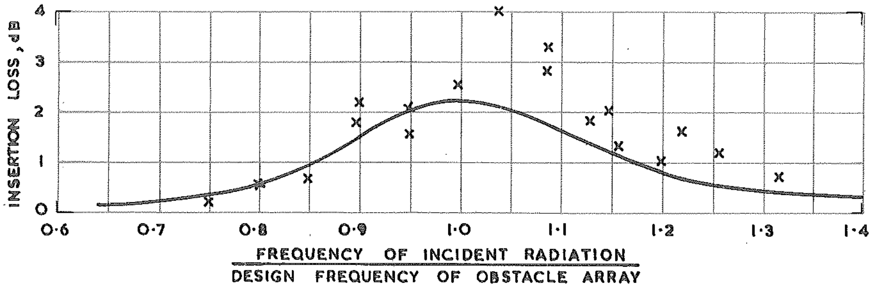

Fig. 22 - Comparison of measured loss and curves derived from the general formula using an HR4/4/1 obstacle array, at various frequencies, with an H4/4/1 source array

× measured points
—— general curve

To determine where an array may be sited so that the insertion loss (L) shall not exceed a given limit (a maximum loss of 1 dB is suggested for a high-power installation), the procedure is as follows:

(i) From equation (3) and the specified value of L ($L = 1$ for 1 dB insertion loss) determine the value of K/L, assuming a likely value for ψ.

(ii) Select Fig. 25, 26 or 27, according to the type of source array. Place the obstacle array so that it lies outside the appropriate K/L contour.

(iii) Note the resulting value of ψ, re-calculate K/L and modify the position of the obstacle if necessary.

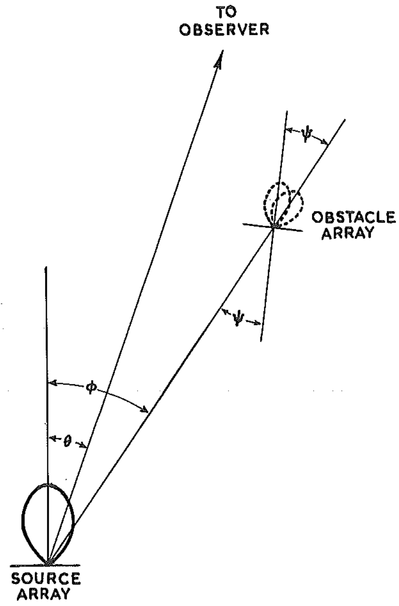

Fig. 23 - Dependence of insertion loss upon h.r.p. of source array

Although the maps give an upper limit to the insertion loss at a given separation, a loss of such magnitude may well occur over part of the service area of the source array. The minimum distance given by the above method is therefore recommended.

If, instead, the insertion loss due to an existing array is required, an upper limit may be determined by finding, from the position of the obstacle on the appropriate map, the corresponding value of K/L. Knowing the value of K, the value of L may be determined.

5.5. The insertion loss due to a large number of obstacle arrays

The experimental results described in this report apply to a single obstacle array. Nevertheless, the general insertion loss formula derived from them may be used to assess the loss which will occur in the practical case when several obstacles are present.

If the obstacle arrays are close to the source only a small number will be strongly illuminated, but their effects will be large and in the worst case will be additive. An estimate of the maximum possible loss which may occur in particular directions can be obtained by adding the individual losses calculated by the method described at the conclusion of Section 5.4.

If many obstacles are capable of intercepting the radiation from the source array, the majority must inevitably be situated at a considerable distance from the source. The lengths of the paths taken by waves travelling viâ the various obstacles to the observer will differ by appreciable fractions of a wavelength, and the re-radiated fields can therefore be considered as having a random phase relationship.

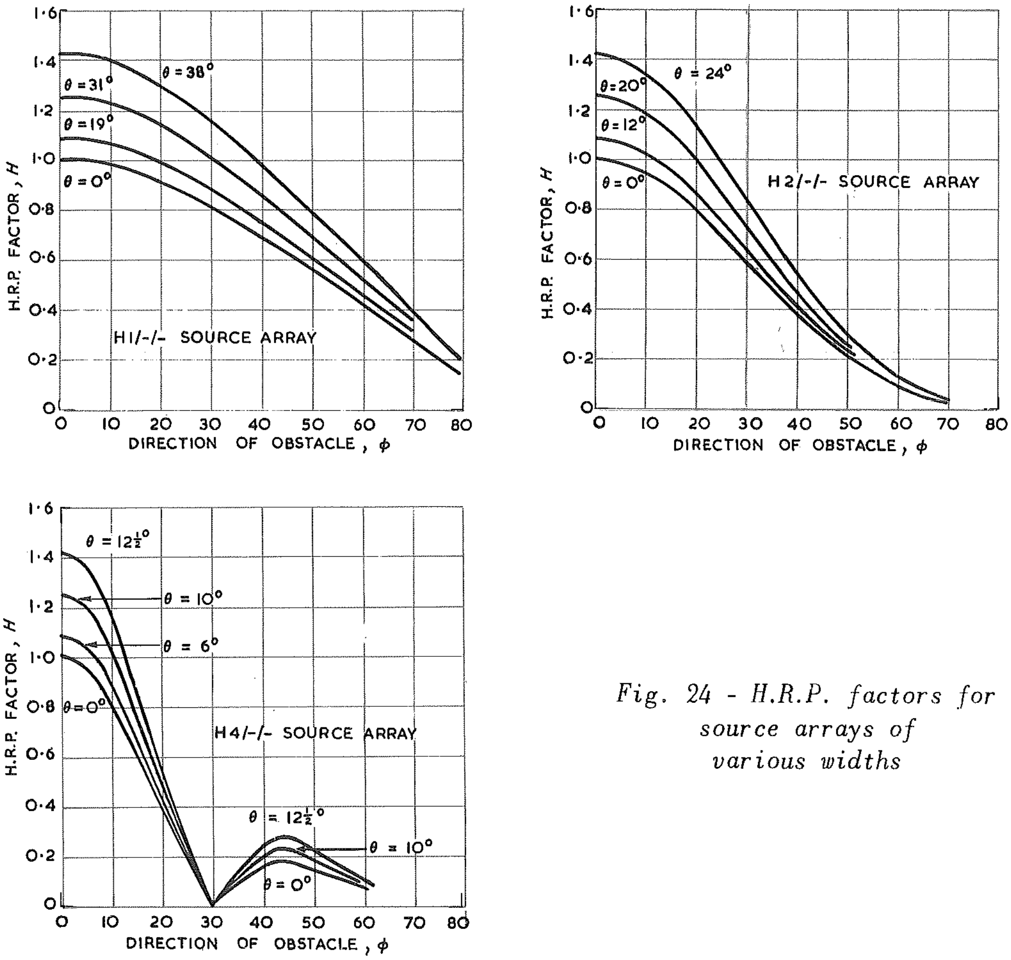

Fig. 24 - H.R.P. factors for source arrays of various widths

The effect of this random phase relationship may be taken into account by assuming that the total loss is the square root of the sum of the squares of the individual losses, each calculated by the method described in Section 5.4.

In practice the loss due to one particular obstacle array (intended for the same frequency band as the source array) often predominates; the total loss is then only slightly greater than the loss of this one array.

6. THE EFFECT OF IONOSPHERIC IRREGULARITY ON THE INSERTION LOSS OF AN OBSTACLE ARRAY

It is well known that signals received from a distant transmitter on two spaced aerials are in general uncorrelated because of ionospheric irregularities. This property is made use of in diversity reception. From the principle of reciprocity, it would appear at first sight that such effects will greatly influence the insertion loss measured at a distant point, because the re-radiation from the obstacle will be randomly related to the signal from the driven array after reflexion from the ionosphere. In diversity reception signals of comparable amplitude received on spaced aerials are combined in such a way that the amplitude of the resulting output

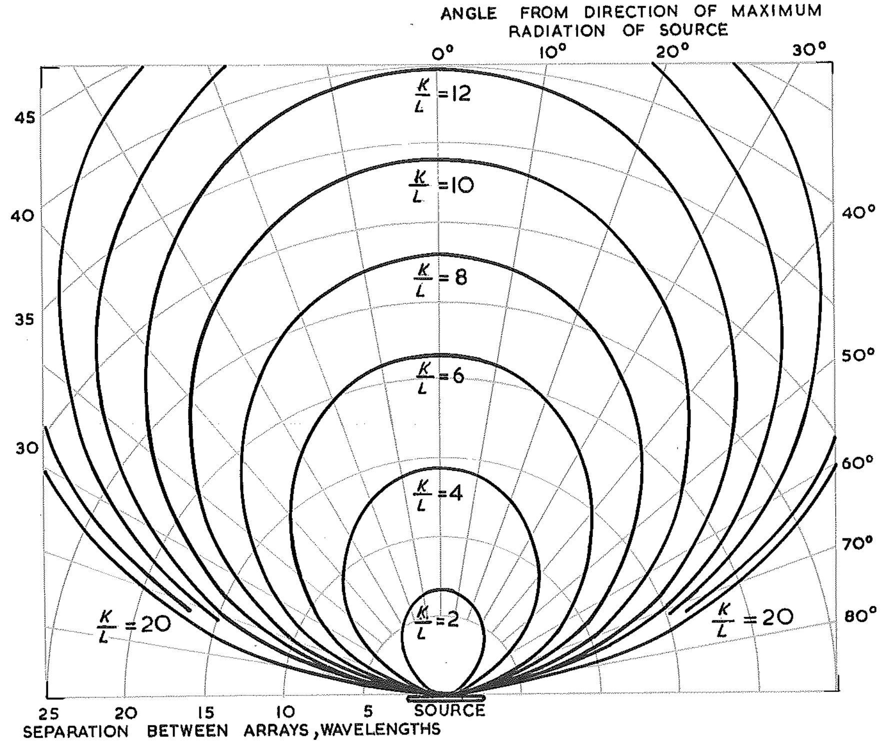

Fig. 25 - Restricted areas, H1/n/h source array

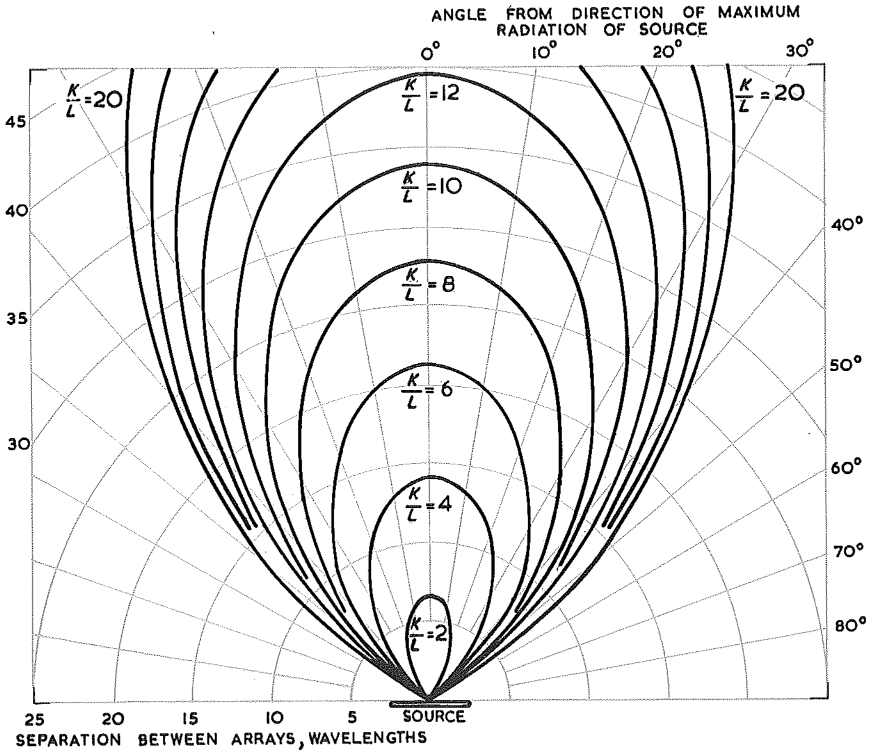

Fig. 26 - Restricted areas, H2/n/h source array

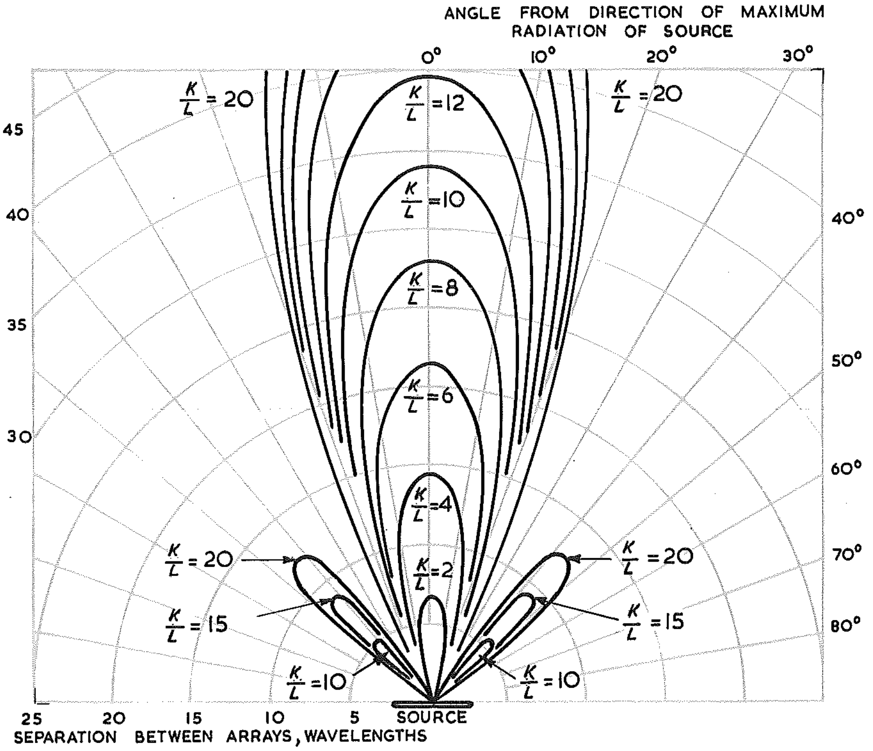

Fig. 27 - Restricted areas, H4/n/h source array

is subject to less variation than that of the individual signals. The reception of a fading signal from an array firing through another array is different, however, because the direct and re-radiated signals are of very different amplitudes and are added in random phase before detection.

Bramley[4] has shown that the diversity effects observed with aerials spaced along the line of propagation are most satisfactorily explained in terms of a 'steady' signal (or specularly reflected component) superimposed on a 'random' background composed of the continuous angular distribution due to diffraction from a relatively rough ionosphere. In the case of transmission in the presence of an obstacle, the ratio of the steady components of the direct and re-radiated signals gives the firing-through loss which would occur with a smooth ionosphere. With a rough ionosphere, we may regard the direct signal as a steady reference signal, since we are concerned with the ratio of the direct and re-radiated signals and not with their absolute values. The re-radiated signal may then be regarded as the sum of a steady signal and random components of similar magnitude contributed from both signals. When the steady component of the re-radiated signal is small compared with the reference signal the random components are even smaller and do not greatly influence the firing-through loss. Calculations based on this theory, using average values for fading (as specified by a 'steady-to-random' power ratio) have shown that the insertion loss for obstacle arrays spaced less than 20λ differs only by a small amount from the free-space value except when severe fading is present; this latter case is of little interest since the main signal itself is then unusable for a broadcasting service.

The direct and re-radiated signals may be less correlated for obstacle separations greater than 20λ, but at these distances, the resulting insertion losses are generally small and fluctuations are relatively unimportant. The effects of ionospheric irregularity can therefore always be disregarded when assessing insertion losses due to obstacle arrays.

7. CONCLUSIONS

The measurements described in this report show that considerable reductions in field strength may occur if arrays operating in the same or adjacent frequency bands are situated close to each other. If, however, the arrays can be suitably disposed, the attenuation may be reduced to an acceptable value. The insertion loss of an obstacle cannot, in general, be determined precisely because of features which are usually unspecified. By using the method derived in Section 5, however, either an upper limit for the loss may be assessed, or the position for an array rapidly determined in order not to exceed a specified insertion loss anywhere within the service area.

8. ACKNOWLEDGEMENTS

The models used in the experiments were constructed by Mr. K.G. Haughton, who, together with Mr. F. Bonar, assisted with the measurements.

9. REFERENCES

1. Page, H., 'The Measured Performance of Horizontal Dipole Transmitting Arrays', Journal I.E.E., Vol. 92, Part III, No. 18, 1945.

2. Morris, D.W., Thurlow, E.W., and Genna, W.N., 'A Microwave Model Equipment for Use in the Study of the Directivity Characteristics of Short-Wave Aerials', The Post Office Electrical Engineers' Journal, Vol. 51, October 1958.

3. Mentzer, J.R., 'Scattering and Diffraction of Radio Waves', pp. 98 and 99, Pergamon Press, 1955.

4. Bramley, E.N., 'Diversity Effects in Spaced-Aerial Reception of Ionospheric Waves', Proc. I.E.E., Vol. 98, Part III, No. 51, January 1951.

5. Schelkunoff, S.A., 'Advanced Antenna Theory', p. 181.

APPENDIX

THE INSERTION LOSS OF A RECTANGULAR OBSTACLE

The accuracy of the measuring system was tested by comparing the measured and theoretical insertion losses caused by rectangular metallic sheets; these comparisons are described in Section 3.2.

The experimental arrangement is shown diagrammatically in Fig. 28 in which the rectangle ABCD represents a rectangular conducting screen, corresponding to the obstacle (and its image). The point P corresponds to the position of one of the elements of the source array. The problem to be solved is that of finding the sum of the contributions to the distant field due to all the elements in the array and their images. This can most easily be done by applying the principle of reciprocity and assuming a distant transmitter since a horizontally-polarized plane wave is then incident on both the source array and the obstacle. The resultant field at the centre of individual elements due to both the plane wave and the re-radiation from the screen may then be determined. The received signal is proportional to the vector sum of the fields at the element centres, the contributions from the elements forming the image being reversed in phase.

This problem will be solved by the use of Fresnel diffraction theory, showing first that edge effects can be disregarded and that the current induced on the obstacle may be taken to be everywhere proportional to the incident field.

It may be shown from Schelkunoff's expression[5] for the field in the vicinity of a wedge that the currents flowing in a half plane (relative to those flowing in a whole plane), due to a plane wave at normal incidence, take the form shown in Fig. 29. The re-radiation from the plane can be assessed by considering the average current density over the plane. The curves of Fig. 30, obtained by integrating between prescribed

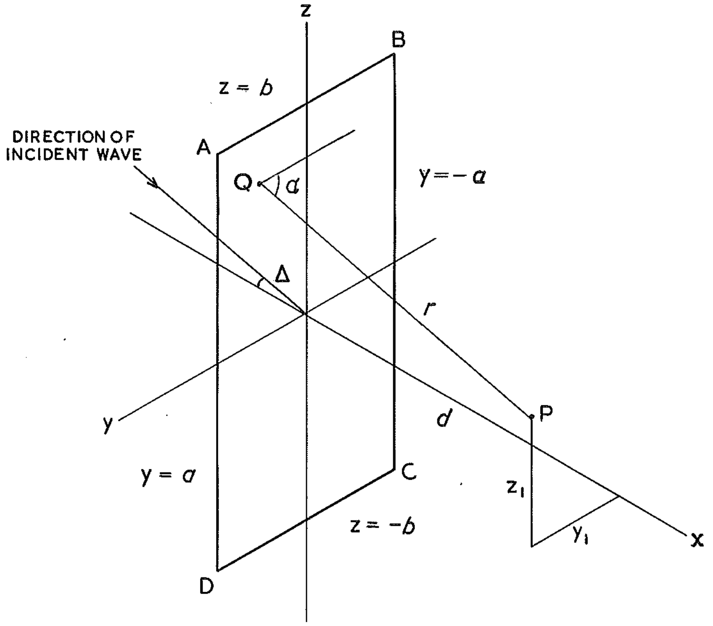

Fig. 28 - A rectangular obstacle

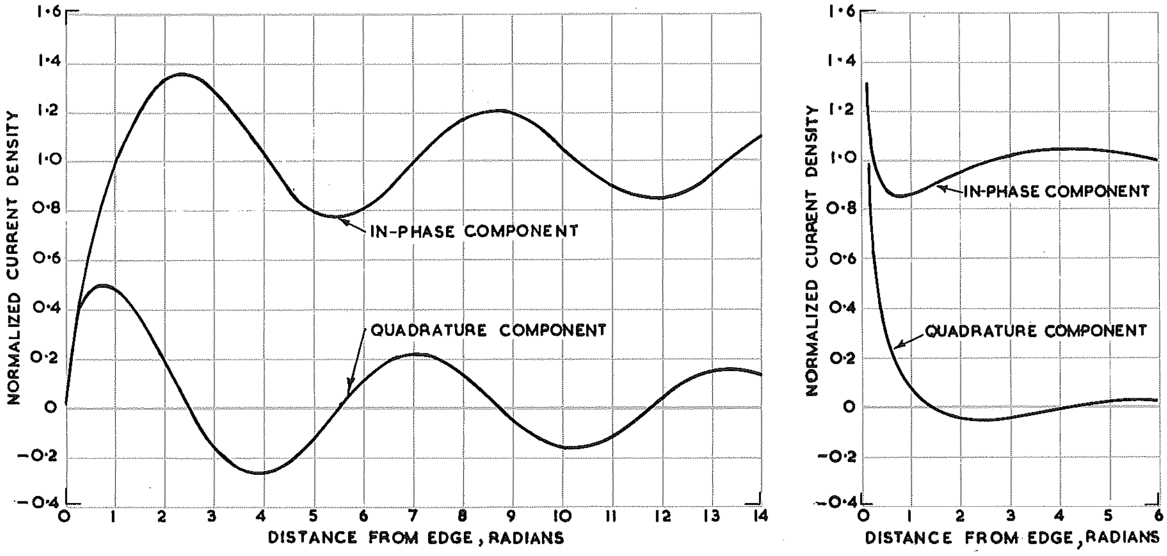

(*a*) (*b*)

Fig. 29 - The current distribution near the edge of a half-plane illuminated by normally-incident radiation

(a) electric vector of incident wave perpendicular to edge
(b) electric vector of incident wave parallel to edge

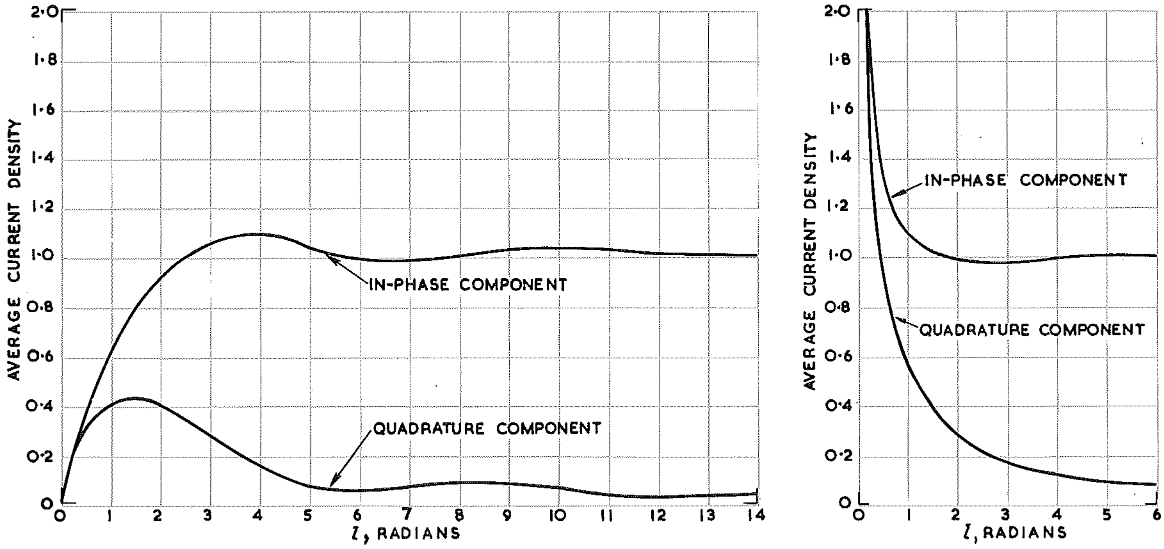

(*a*) (*b*)

Fig. 30 - The average current density between the edge of a half-plane and a parallel line distant l from it, for normally-incident radiation

(a) electric vector of incident wave perpendicular to edge
(b) electric vector of incident wave parallel to edge

limits the curves of Fig. 29, show the current density averaged over the area between the edge and a line spaced l from it. Taking this line to correspond to each of the two axes of symmetry of the screen (and its image) in turn, an estimate of the current density averaged over the whole of the screen (and its image) may be obtained. For the smaller of the two screens (2λ wide and - with its image - 5λ high) the curves of Fig. 30 show that the average current density across its width is $0{\cdot}98 + j0{\cdot}06$; over its height it is substantially equal to unity. Thus the overall average current density does not differ from the corresponding value for an infinite plane by more than 7%; the corresponding figure for the larger obstacle (3·43λ wide and 7·04λ high with image) is 5%. These figures apply to normally-incident radiation but they would be expected to be substantially the same for waves incident at a small angle to the normal. The field re-radiated from screens of these sizes may therefore be calculated by assuming them to form part of an infinite screen.

Consider a conducting screen in the $x = 0$ plane (Fig. 28), bounded by the lines $y = \pm a$, $z = \pm b$. Suppose a horizontally-polarized plane wave, the direction of propagation of which lies in the $y = 0$ plane and makes an angle Δ with the x axis, is incident upon the screen. Then the density of the current induced on the screen is equal to the tangential magnetic component of the incident field; this is equal to $2H\cos\Delta$, where H is the magnetic intensity which the incident wave would have in the $x = 0$ plane if the screen were removed. Now $H = E/\eta_0$, where E is the electric intensity of the incident wave and η_0 is the intrinsic impedance of free space. The electric intensity in the $x = 0$ plane (in the absence of the screen), normalized to the electric intensity at the origin, is described by

$$E = \exp\,(j\beta z\,\sin\Delta) \tag{6}$$

where $\beta = 2\pi/\lambda$. Thus the surface current density on the screen is given by

$$J = 2H\cos\Delta = \frac{2}{\eta_0}\cos\Delta\,\exp(j\beta z\,\sin\Delta) \tag{7}$$

The electric intensity at P due to the current flowing in an elementary area of the screen at Q is

$$\delta E_R = j\eta_0\,\frac{J\sin\alpha\,\exp(-j\beta r)}{2\lambda r}\,\delta y\;\delta z \tag{8}$$

where $r = PQ$ ($r \gg \lambda$) and α is the angle between PQ and the direction of current flow. Combining equations (7) and (8) gives, for the total re-radiated field

$$E_R = \frac{j\cos\Delta}{\lambda}\iint\frac{1}{r}\,\sin\alpha\,\exp\left[j\beta(z\,\sin\Delta - r)\right]dy\;dz \tag{9}$$

When the distance between the obstacle and the point P is sufficiently large we may write $\sin\alpha \simeq 1$ and assume that the inverse distance term is constant and equal to $1/d$. For the exponents, however, it is necessary to write

$$r \simeq d + \frac{1}{2d}(y - y_1)^2 + \frac{1}{2d}(z - z_1)^2$$

where d, y_1, z_1 are the co-ordinates of P; both y_1 and z_1 are small compared with d. Making these substitutions it may be shown that

$$E_R = \frac{j}{\lambda d} \cos\Delta \exp\left[j\beta(z_1 \sin\Delta + \frac{d}{2} \sin^2\Delta - d)\right] I_1 I_2$$

where
$$I_1 = \int_{-a}^{a} \exp\left[-\frac{j\beta}{2d} (y - y_1)^2\right] dy$$

and
$$I_2 = \int_{-b}^{b} \exp\left[-\frac{j\beta}{2d} (z - z_1 - d \sin\Delta)^2\right] dz \qquad (10)$$

I_1 and I_2 may be expressed in terms of Fresnel integrals by making the substitutions:-

$$v = (y - y_1) \left(\frac{2}{\lambda d}\right)^{\frac{1}{2}} \text{ and } w = (z - z_1 - d \sin\Delta) \left(\frac{2}{\lambda d}\right)^{\frac{1}{2}}$$

Thus, putting $(1 - \frac{1}{2} \sin^2\Delta) \simeq \cos\Delta$, we have

$$E_R \simeq j\frac{\cos\Delta}{2} \exp\left[-j\beta(d \cos\Delta - z_1 \sin\Delta)\right] \int_{v_1}^{v_2} \exp(-j\frac{\pi v^2}{2}) dv \int_{w_1}^{w_2} \exp(-j\frac{\pi w^2}{2})\, dw \qquad (11)$$

where
$$v_1 = -(y_1 + a) \left(\frac{2}{\lambda d}\right)^{\frac{1}{2}} \qquad w_1 = -(z_1 + d \sin\Delta + b) \left(\frac{2}{\lambda d}\right)^{\frac{1}{2}}$$

$$v_2 = -(y_1 - a) \left(\frac{2}{\lambda d}\right)^{\frac{1}{2}} \qquad w_2 = -(z_1 + d \sin\Delta - b) \left(\frac{2}{\lambda d}\right)^{\frac{1}{2}}$$

The phase of the re-radiated field may be referred to the point $(d, 0, 0)$ by multiplying by $\exp(j\beta d \cos\Delta)$; it is convenient to do this since this point is usually assumed as the phase centre of the array. The expression for the re-radiated field then becomes

$$E'_R = \frac{j\cos\Delta}{2} \exp(j\beta z_1 \sin\Delta) \int_{v_1}^{v_2} \exp(-j\frac{\pi v^2}{2})\, dv \int_{w_1}^{w_2} \exp(-j\frac{\pi w^2}{2})\, dw \qquad (12)$$

The direct field at P referred to the point $(d, 0, 0)$ is

$$E'_D = \exp\,(j\beta z_1 \sin\Delta) \qquad (13)$$

Equations (12) and (13) may be applied in turn to the points corresponding to the centres of all the elements of the array and their images. The total voltage induced in the array is then proportional to the sum of the contributions from the individual elements, the contributions from the image elements being added in antiphase. Having calculated the total effect of the direct and re-radiated fields, the resultant induced voltage and hence the insertion loss of the obstacle may be determined.

ALG

Printed by B.B.C. Research Department, Kingswood Warren, Tadworth, Surrey